forests

MDPI

Article

Technological Properties of Some Non-Native Hardwood in Mediterranean Area

Antonio Zumbo [1], Angela Lo Monaco [2,*], Salvatore F. Papandrea [1], Rodolfo Picchio [2] and Andrea R. Proto [2]

[1] Department of AGRARIA, Mediterranean University of Reggio Calabria, Feo Di Vito Snc, 89122 Reggio Calabria, Italy; antonio.zumbo@unirc.it (A.Z.); salvatore.papandrea@unirc.it (S.F.P.)
[2] Department of Agriculture and Forest Sciences, University of Tuscia, Via San Camillo de Lellis, Snc, 01100 Viterbo, Italy; r.picchio@unitus.it (R.P.); andrea.proto@unirc.it (A.R.P.)
* Correspondence: lomonaco@unitus.it

Abstract

A growing global demand for wood, coupled with the role of this material in low-carbon strategies, is fuelling interest in fast-growing plantations, including short-rotation forestry (SRF) and agroforestry systems. However, evidence of the physical–mechanical properties and possible uses of non-native hardwoods in the Mediterranean environment remains limited. This study aimed to address this current knowledge gap by evaluating the main physical and mechanical properties of six fast-growing non-native tree species cultivated in experimental plots in Calabria, southern Italy. The wood of *Eucalyptus occidentalis* Endl., *E.* × *trabutii* (M. Vilm. ex Trab.) A. Chev., *E. camaldulensis* Dehnh., *E. bridgesiana* R.T.Baker, *Melia azedarach* L., and *Paulownia tomentosa* (Thunb.) Steud., were evaluated. The dynamic elastic modulus (MOE_d) was estimated on standing trees using stress waves (TreeSonic™). In the laboratory, swelling and shrinkage (ISO 13061-14 and 16), static modulus of elasticity (MOE_s) and modulus of rupture (MOR) (EN 408), and compressive strength (ISO 13061-16) were determined. The data were analysed using one-way ANOVA, followed by Tukey's HSD test where appropriate. Swelling and shrinkage showed no significant differences ($p > 0.05$). One-way ANOVA revealed a significant effect of species on MOE_s ($p < 0.001$). Both standing-tree stress-wave measurements (MOE_d) and laboratory tests (MOE_s, MOR, and compression strength) revealed significant variability in stiffness and resistance among the species examined. The positive relationship observed between MOE_d and MOE_s indicates that stress-wave testing can serve as a practical, rapid tool for ranking plantation material at an early stage, thereby supporting early decision-making in SRF and agroforestry systems. These results provide comparative evidence for species and clonal selection, and to optimise the allocation of plantation resources to targeted value chains in Mediterranean environments.

Keywords: physical properties; dynamic modulus of elasticity; static modulus of elasticity; modulus of rupture; *Eucalyptus* sp.; *Melia azedarach*; *Paulownia tomentosa*; fast-growing plantation

Academic Editors: Goran Mihulja, Tomislav Sedlar, Murco Obucina and Chandan Kumar

Received: 10 March 2026
Revised: 23 March 2026
Accepted: 27 March 2026
Published: 1 April 2026

1. Introduction

Wood is a renewable, multifunctional resource that plays an increasingly important role in low-carbon strategies, owing to its potential for carbon storage and as substitution for more emission-intensive materials. Its combination of structural efficiency, durability, and versatility has supported its use for centuries in construction, furniture, tools, and fuels [1]. Also, its aesthetic beauty is obvious, as seen in its extensive use for veneers, floorings, frames and furniture [2].

Global wood demand has been rising steadily over the last few years, with an average annual growth of about 1.1% [3]. Several forecasts suggest that this pace may accelerate in the coming decades [4,5]. The expected increase is linked to well-known drivers, including demographic trends, economic development, and the growing role of wood and other bio-based materials in pathways toward net-zero emissions [6,7]. In terms of supply, current scenarios predict a 4%–8% expansion in global roundwood production over the 2022–2030 period, indicating moderate growth in the short term [8]. By 2050, roundwood production could rise by 6%–32% relative to 2022, with an absolute increase ranging from roughly 240 to 1200 million m^3, depending on the scenario [8].

In this context, to help meet the high and growing demand for wood for multiple end-uses, fast-growing plantations have become an important source of feedstock for the pulp and paper sector and can provide biomass for energy and biofuels, while also delivering additional benefits such as land restoration and the mitigation of desertification processes [9,10]. Two complementary fast-growing plantation-based approaches are increasingly considered to expand sustainable wood supply while enhancing land multifunctionality: short-rotation forestry (SRF), primarily aimed at rapid biomass and small-roundwood production, and agroforestry plantations, which integrate trees with crops and/or livestock to deliver both production and ecosystem-service benefits. In particular, short-rotation forestry (SRF) broadly refers to the establishment of high-density plantations of fast-growing tree species managed under relatively short cycles to supply woody biomass and/or small diameter roundwood [11]. Two operational concepts are denoted: short-rotation coppice (SRC), where the trees are harvested in short intervals (2–8 years) to produce biomass [12], and SRF systems, managed on longer short turns (10–20 years) to obtain small-diameter logs [13]. Such species have been introduced in various regions worldwide due to their rapid growth, adaptability, and potential economic returns [14].

In Europe, the species most frequently considered for SRF/SRC include willows (*Salix* spp.), poplars (*Populus* spp.), and black locusts (*Robinia pseudoacacia* L.), while other fast-growing species may include *Eucalyptus* spp. [15].

On the other hand, interest in agroforestry plantations is increasing. This system integrates tree species with agricultural and/or animal production, in spatial or temporal arrangements that promote ecological and economic interactions [16,17]. Furthermore, agroforestry systems (AFS) have increasingly attracted producers because they can generate diversified outputs: short-term returns from annual crops, medium-term products such as fruits, nuts, and green biomass, and long-term products, including fibre, pulpwood, timber, and fuelwood, thereby enhancing overall farm profitability and increasing land value [16,18–20].

Species selection in agroforestry is strongly context-dependent; nevertheless, European plantations frequently employ valuable hardwoods such as walnut (*Juglans nigra* L.) [21], wild cherry (*Prunus avium* L.), and fruit trees in diversified farm systems [22], and can also involve olive-based plantations. Among non-native species in Europe, examples reported in agroforestry-oriented plantings include mindi (*Melia azedarach* L.) [23] and paulownia (*Paulownia tomentosa* (Thunb.) Steud) [24].

Tree growth, wood formation, and wood quality are influenced by stand density and spacing, as well as by competition for light, nutrients, and water [16,25]. These constraints can be especially relevant in SRF and are even more complex in agroforestry, where trees and crops differ in physiological requirements and resource-demand patterns [26,27].

Despite the growing interest in fast-growing and non-native hardwood species for Mediterranean environments, studies specifically addressing their physical and mechanical properties and potential industrial uses remain limited [28–33]. Considering the potential

role of fast-growing species, this study aimed to fill the existing knowledge gap by evaluating the main physical and mechanical properties of selected fast-growing, non-native tree species in a Mediterranean experimental clonal plantation and by providing comparative evidence to support their potential use in plantation systems. In addition, the study assessed the relationship between the dynamic modulus of elasticity (MOE_d), obtained from stress-wave measurements on standing trees, and the static modulus of elasticity (MOE_s), measured in bending tests, to evaluate the suitability of non-destructive techniques for predicting and ranking elastic performance across the investigated clones.

2. Materials and Methods

2.1. Experimental Site and Wood Sampling

The wood material used in this study was collected from the ARSAC (Regional Company for the Development of Calabrian Agriculture) experimental clonal plot of fast-growing plantations located in the municipality of Rocca di Neto (Crotone Province), Calabria region, southern Italy. Regarding the climatic regime of the study area, it is characterised by a hot-summer Mediterranean climate, with a marked seasonal contrast between a dry, predominantly clear summer and a wetter, windier, partly cloudy winter. Air temperature typically ranges from about 7 to 32 °C, rarely falling below 3 °C or exceeding 35 °C. Precipitation (annual mean 571 mm) shows strong seasonality, with a wetter season extending roughly from late September to April and a pronounced summer minimum.

In particular, the wood species examined were *Eucalyptus occidentalis* Endl., *Eucalyptus* × *trabutii* H. Vilm, *Eucalyptus camaldulensis* Dehnh., *Eucalyptus bridgesiana* R. T. Baker, *Melia azedarach* L., and *Paulownia tomentosa* (Thunb.) Steud. The plantations were established in 2011, with an experimental area of 0.20 hectares for each species. The short-rotation forestry of *Eucalyptus* species has a square layout and tree space of 3 × 2 m. Similarly, the agroforestry plantation of *Melia* and *Paulownia* were established with a spacing of 3 × 2 m. The characteristics of each species are present in Table 1.

Table 1. Characteristics of clonal plantations.

Species	Square Layout (m)	Mean DBH (cm)	Mean Height (m)	Basic Density (kg/m^3)
Eucalyptus occidentalis	3 × 2	24	14.8	544.22 ± 19.45
Eucalyptus × *trabutii*	3 × 2	28	14.6	517.42 ± 22.00
Eucalyptus camaldulensis	3 × 2	17	15.2	454.61 ± 30.32
Eucalyptus bridgesiana	3 × 2	33	16.5	562.29 ± 36.88
Melia azedarach	3 × 2	26	14.5	551.43 ± 36.26
Paulownia tomentosa	3 × 2	39	12.8	223.59 ± 18.70

Note: DBH = diameter at breast height.

From each species, the logs were selected and transported to the Laboratory of Wood Technology of the AGRARIA Department of Reggio Calabria to produce specimens for physical and mechanical tests. Specimens were cut from a 1 m length log of trees (from 0.3 to 1.3 m height above the ground). Only clear wood specimens, free from visible defects such as knots, checks, reaction wood, or other irregularities in the sampled area, were used for the physical and mechanical investigations.

Small clear specimens were prepared, labelled and conditioned in a climatic chamber (Memmert 750 Eco, GmbH, Schwabach, Germany; with temperature accuracy of 0.1 °C and humidity accuracy of 0.5% RH) at 20 °C (±2) and 65% (±5) RH until they reached an equilibrium moisture content (EMC) of 12%. The air-dried density of each specimen

was measured following ISO 13061-2:2014 [34], while moisture content was determined through oven drying in accordance with ISO 13061-1:2014 [35].

2.2. Determination of Dynamic Modulus of Elasticity (MOE_d)

The dynamic modulus of elasticity was determined on standing trees, using the TreeSonic™ (Fakopp Enterprise, Agfalva, Sopron, Hungary). This instrument measures the propagation time of sound waves along the length of wood fibres. The TreeSonic™ device consists of a handheld impact hammer and two sensor probes equipped with a transmitting and a receiving accelerometer. Measurements were performed by inserting the two probes (transmitter and receiver) into the sapwood and generating an acoustic pulse through a hammer impact, which introduced the stress wave into the stem. The probes were positioned on the same side of the tree and aligned within a vertical plane, with a 1.00 m measurement span approximately centred at breast height and the lower probe located about 60–70 cm above the forest floor. For each selected tree, three readings were taken and the mean transit time was used for subsequent calculations. To determine wave velocity, both probes were driven through the bark into the wood at an angle of 45°, consistent with the instrument design for longitudinal measurements. Acoustic velocity was computed from the probe spacing and the corresponding time-of-flight (TOF) according to Equation (1):

$$v = S/TOF \quad (1)$$

where v = tree acoustic velocity (m/s), S = distance between sensors (m), TOF = time of flight (s).

For the determination of the MOE_d, wood density was measured on representative specimens for each species, collected from the same trees and from stem positions corresponding to the measurement range of the acoustic test. These values were used as species-level input for the stress-wave model to ensure consistency between density specimens and standing-tree acoustic measurements. Wood density was determined at the Laboratory of Wood Technology of the AGRARIA Department of Mediterranean University of Reggio Calabria.

Afterwards, it was possible to calculate the dynamic modulus of elasticity (MOE_d) according to Equation (2):

$$MOE_d = \rho \times v^2 \quad (2)$$

where MOE_d = dynamic modulus of elasticity (GPa), ρ = tree wood density (kg/m^3), and v = tree acoustic velocity (m/s).

2.3. Determination of Swelling and Shrinkage of Wood

The determination of swelling and shrinkage properties of wood were calculated in accordance with the ISO 13061-16:2025 [36] and ISO 13061-14:2024 [37]. The specimens for this test had dimension of 2 × 2 × 3 cm (R × T × L). For the total swelling coefficient (α_{max}), the specimens were measured along the three anatomical directions with an accuracy of 0.01 mm. The specimens were then completely immersed in distilled water, and their mass and dimensions were periodically re-measured until the variation between two consecutive measurements was lower than 0.5%, which was assumed to indicate that maximum constant dimensions (saturation) had been reached. The volumetric total swelling coefficient was calculated according to Equation (3):

$$\alpha_{max} = \frac{(V_{max} - V_0)}{V_0} \times 100 \quad (3)$$

where α_{max} = volumetric swelling (%), V_{max} = volume of specimens saturated, V_0 = volume of anhydrous specimens.

The same specimens were subsequently used to determine the total shrinkage coefficients (β_{max}). After the immersion phase, the wet specimens were air-conditioned for a few days and then oven-dried at 103 ± 2 °C to constant mass. The volumetric total shrinkage coefficient was calculated according to Equation (4):

$$\beta_{max} = \frac{(V_{max} - V_0)}{V_{max}} \times 100 \quad (4)$$

where β_{max} = volumetric shrinkage (%), V_{max} = volume of saturated specimens, V_0 = volume of anhydrous specimens.

2.4. Determination of the Static Modulus of Elasticity and the Modulus of Rupture

The static modulus of elasticity (MOE_s) and modulus of rupture (MOR) were determined perpendicular to the grain (Figure 1). A four-point bending test was performed in accordance with EN 408:2010+A1 (2012) [38] using a 300 kN universal testing machine (METRO COM, Garbagna Novarese (NO), Italy–model 10402030). Data were recorded using the dedicated METRO COM software Dina 960 xp. The length of the specimen was 21 times its width. The supports were placed at a distance equal to 18 times the width, and the two load points were placed at a distance from each support equal to 6 times the width. During the tests, the load and the bend values were registered. The specimens had a square cross-section with a side of 2 cm, and length equal to 42 cm. The distance between the two loading points was 12 cm, while the distance between the two supports was 36 cm. The feed rate of the crosshead was 3.6 mm/min.

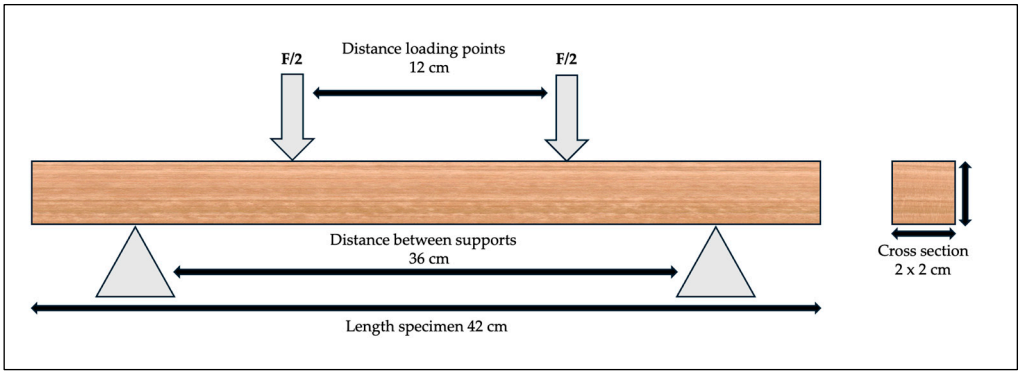

Figure 1. Schematic representation of the four-point bending test configuration used for the determination of MOE_s and MOR.

2.5. Determination of Compression Strength

In the same laboratory, a compressive strength test was performed following ISO 13061-17:2022 [39]. The specimens had a square cross-section with a side length of 2 cm. The length, parallel to the grain, was 3 cm. The maximum load was reached between 1 and 5 min after loading began, with a feed speed of 5 mm/min. The compressive strength was measured using Equation (5):

$$C = \frac{F_{max}}{A} \quad (5)$$

where C = compressive strength parallel to the grain (N/mm^2); F_{max} = maximum load (N); A = cross-sectional area (mm^2).

2.6. Statistical Analysis

Statistical analyses were conducted in R (version 4.5.2) (R Foundation for Statistical Computing, Vienna, Austria). For each response variable, species differences were assessed using one-way ANOVA ($\alpha = 0.05$), followed by Tukey's HSD test. Effect size was reported as omega-squared (ω^2). The normality of residuals and homogeneity of variances were assessed using the Shapiro–Wilk and Levene tests, respectively. Stress-wave variables (time-of-flight, velocity, and MOE_d) were analysed similarly. The relationship between MOE_d and static MOE was investigated using paired observations; when multiple specimens shared the same MOE_d within a species, static MOE was averaged to avoid pseudo-replication.

3. Results and Discussion

3.1. Statistical Analysis Results

For each response variable, a one-way ANOVA was performed to test for interspecific differences, and Tukey's HSD was used for post hoc comparisons when the overall test was significant. The ANOVA outcomes for the main response variables are summarised in Table 2 and are referenced throughout the following subsections.

Table 2. Summary of one-way ANOVA results and effect sizes (ω^2) for the investigated response variables.

Property	N	df1	df2	F	*p*-Value	ω^2
MOE_d	120	5	114	296.46	<0.001	0.925
Shrinkage	72	5	66	0.44	0.816	0.000
Swelling	72	5	66	1.03	0.407	0.002
MOE_s	120	5	114	31.93	<0.001	0.563
MOR	120	5	114	31.54	<0.001	0.560
Compression	180	5	174	196.44	<0.001	0.844

3.2. Dynamic Modulus of Elasticity

Table 3 reports the stress wave times measured on the sample trees and the corresponding wave velocity and dynamic modulus of elasticity. Stress-wave measurements revealed clear differences between species in terms of both wave propagation velocity and dynamic elastic modulus (MOE_d). The highest velocity was recorded in *Melia azedarach* (3889 ± 175 m/s), which also showed the highest MOE_d (11.37 ± 1.03 GPa). High values were also observed in *Eucalyptus* × *trabutii*, characterised by mean velocities of 3292 ± 87 m/s and a MOE_d of 10.30 ± 0.54 GPa, with relatively limited variability. *Eucalyptus occidentalis* showed intermediate levels, with velocities of 2903 ± 140 m/s and a mean MOE_d of 9.42 ± 0.92 GPa. Conversely, *Eucalyptus camaldulensis* showed lower velocities (2548 ± 126 m/s) and a lower MOE_d (7.49 ± 0.73 GPa). *Eucalyptus bridgesiana* showed a low velocity and MOE_d of 2593 ± 134 m/s and 6.40 ± 0.66 GPa, respectively; in contrast, *Paulownia tomentosa* showed the lowest MOE_d (5.75 ± 0.56 GPa), despite a relatively high velocity of 3199 ± 153 m/s.

Table 3. Stress-wave measurements and derived dynamic properties of the investigated tree species.

Tree Species	Wood Density (kg/m^3) Mean	Stress Wave Time (µs) Mean ± SD	Wave Velocity (m/s) Mean ± SD	MOE_d (GPa) Mean ± SD
Eucalyptus occidentalis	1115	345 ± 16	2903 ± 140	9.42 ± 0.92 c
Eucalyptus × *trabutii*	950	304 ± 8	3292 ± 87	10.30 ± 0.54 b
Eucalyptus camaldulensis	1150	393 ± 19	2548 ± 126	7.49 ± 0.73 d
Eucalyptus bridgesiana	950	386 ± 20	2593 ± 134	6.40 ± 0.66 e
Melia azedarach	750	257 ± 11	3889 ± 175	11.37 ± 1.03 a
Paulownia tomentosa	560	313 ± 14	3199 ± 153	5.75 ± 0.56 f

Note: Within the column MOE_d, means sharing the same letter are not significantly different (Tukey's HSD, $\alpha = 0.05$).

One-way ANOVA indicated a significant effect of species on MOE_d ($F(5, 114) = 296.46$, $p < 0.001$), with a very large effect size ($\omega^2 = 0.925$; Table 2). Tukey's HSD post hoc test (Table 3) ranked the species into distinct groups (a–f), identifying *Melia azedarach* as the highest MOE_d group, followed by *Eucalyptus* × *trabutii* and *Eucalyptus occidentalis*. Lower MOE_d groups included *Eucalyptus camaldulensis* and *Eucalyptus bridgesiana*, whereas *Paulownia tomentosa* consistently exhibited the lowest MOE_d.

Van Duong and Ridley-Ellis [30] determined the dynamic modulus of elasticity (MOE_d) in ten-year-old *Melia azedarach* trees. They reported a MOE_d of 9.9 GPa, which is comparable to the value found in this study (11.37 GPa). Amer et al. [30] observed the dynamic modulus of elasticity on specimens from two Eucalyptus clones (*E. camaldulensis* and *E. grandis*) conditioned at 12% moisture content, reporting values of 17.9 GPa and 10.5 GPa, respectively. The ranking observed for MOE_d among species primarily reflects differences in green wood density and internal stem structure, both of which influence stress-wave propagation and, consequently, the estimated dynamic stiffness.

3.3. Swelling and Shrinkage

Swelling and shrinkage were analysed to provide a comparative overview among species (Table 4). The volumetric total swelling coefficient (α_{max}) ranged from 7.82% to 15.03%, while the volumetric total shrinkage coefficient (β_{max}) ranged from 7.18% to 12.77%. Among the species analysed, *Eucalyptus camaldulensis* showed the highest swelling values (15.03% ± 9.26), whereas the highest shrinkage value was observed in *Melia azedarach* (12.77% ± 1.94). Relatively high swelling values were also found in *Melia azedarach* (14.69% ± 2.63) and *Eucalyptus bridgesiana* (14.39% ± 3.60), while *Eucalyptus occidentalis* showed a swelling equal to 13.75% ± 2.93. Conversely, the lowest values were observed in *Paulownia tomentosa*, with swelling of 7.82% ± 3.25 and shrinkage of 7.18% ± 2.60, followed by *Eucalyptus* × *trabutii* (swelling 12.28% ± 3.70; shrinkage 10.82% ± 3.20). However, one-way ANOVA did not reveal significant differences among species for either shrinkage ($F(5, 66) = 0.44$, $p = 0.816$; $\omega^2 = 0.000$) or swelling ($F(5, 66) = 1.03$, $p = 0.407$; $\omega^2 = 0.002$). In Ukraine, in a plantation of *Paulownia tomentosa* of 10 years, Ivaniuk et al. [40] reported a radial shrinkage of 2.4%, a tangential shrinkage of 3.6%, and a volumetric shrinkage of 5.9%. Tamantini et al. [32], in a technological characterisation based on samples *of Eucalyptus camaldulensis* collected from windbreak strips in Tarquinia (central Italy), reported radial shrinkage ranging from 4.7% to 7.4% (mean 5.8%), a mean tangential shrinkage of 8.4%, and the corresponding volumetric shrinkage was equal to 14.2%, while Serenini et al. [29] investigated radial, tangential, and volumetric shrinkage of *Eucalyptus camaldulensis* from 5-year-old plantations in Mato Grosso (Brazil), reporting values of 6.04%, 8.89%, and 14.49%, respectively. Ferreira et al. [41] investigated the impact of three different levels

of sun exposure on the quality of 5-year-old *Eucalyptus urophylla* × *Eucalyptus grandis* plantations, analysing samples from each exposure level as separate treatments.

Table 4. Volumetric percentage and statistical comparison of swelling and shrinkage of investigated species.

Tree Species	Swelling (%) Mean ± SD	Shrinkage (%) Mean ± SD
Eucalyptus occidentalis	13.75 ± 2.93	12.03 ± 2.31
Eucalyptus × *trabutii*	12.28 ± 3.70	10.82 ± 3.20
Eucalyptus camaldulensis	15.03 ± 9.26	12.59 ± 6.48
Eucalyptus bridgesiana	14.39 ± 3.60	12.51 ± 2.65
Melia azedarach	14.69 ± 2.63	12.77 ± 1.94
Paulownia tomentosa	7.82 ± 3.25	7.18 ± 2.60

Note: No significant differences were detected among species (ANOVA, $p > 0.05$).

They reported a volumetric shrinkage of 9.53% for the conventional plantation. Considering the different exposures, the mean volumetric shrinkage was found to be 9.96%. These values are comparable to those reported in the literature: volumetric shrinkage for native *Eucalyptus camaldulensis* is typically around 14.2% [42], which is close to the mean value measured in the present study (12.59%).

3.4. Static Modulus of Elasticity (MOE_s) and Modulus of Rupture (MOR)

Static modulus of elasticity (MOE_s) showed marked differences between the analysed species (Figure 2A). The highest values were observed in *Eucalyptus* × *trabutii* (12,695 MPa ± 3061), which also showed wide variability, indicating a greater dispersion of results than the other species. Medium-high values were also found in *Melia azedarach* (11,583 MPa ± 2273), with an overall higher distribution than the other species, but with equally significant variability. *Eucalyptus occidentalis* (10,382 MPa ± 2316) showed intermediate values, while *Eucalyptus bridgesiana* (8438 MPa ± 2066) was at a medium-low level. The lowest values were recorded in *Eucalyptus camaldulensis* (7166 MPa ± 1564) and in *Paulownia tomentosa* (5284 MPa ± 718), which showed the lowest MOE_s with relatively limited dispersions.

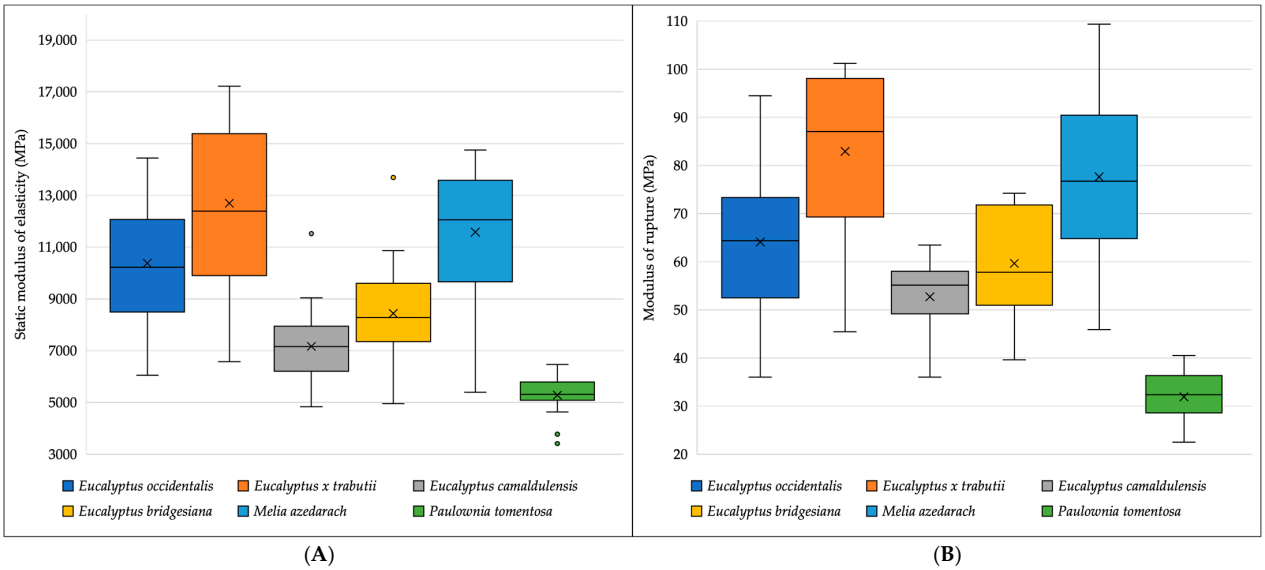

Figure 2. Static modulus of elasticity (**A**) and rupture (**B**) of the investigated species. Coloured dots represent outliers.

One-way ANOVA revealed a significant effect of species on MOE_s ($F(5, 114) = 31.93$, $p < 0.001$), with a large effect size ($\omega^2 = 0.563$; Table 2). Tukey's HSD post hoc test (Table 5) indicated that *Eucalyptus* × *trabutii* belonged to the highest group ("a") and did not differ significantly from *Melia azedarach* ("ab"). *Eucalyptus occidentalis* ("bc") overlapped with *Melia azedarach* and with the intermediate group represented by *Eucalyptus bridgesiana* ("cd"). *Eucalyptus camaldulensis* ("de") was significantly lower than *Eucalyptus occidentalis* and overlapped with *Eucalyptus bridgesiana*, while *Paulownia tomentosa* formed the lowest group ("e").

Table 5. Mean values, standard deviations, and statistical comparison of modulus of elasticity and rupture.

Tree Species	MOE_s (MPa) Mean ± SD	MOR (MPa) Mean ± SD
Eucalyptus occidentalis	10,382.93 ± 2316.08 bc	64.10 ± 17.15 bc
Eucalyptus × *trabutii*	12,695.99 ± 3061.23 a	82.93 ± 17.36 a
Eucalyptus camaldulensis	7166.62 ± 1564.34 de	52.74 ± 7.37 c
Eucalyptus bridgesiana	8438.78 ± 2066.16 cd	59.67 ± 11.67 c
Melia azedarach	11,583.17 ± 2273.72 ab	77.63 ± 19.61 ab
Paulownia tomentosa	5284.90 ± 718.81 e	31.93 ± 4.92 d

Note: Within each column, means sharing the same letter are not significantly different (Tukey's HSD, $\alpha = 0.05$).

Instead, the modulus of rupture (MOR) showed a trend similar to that observed for the MOE_s, highlighting differences between species (Figure 2B). Overall, *Eucalyptus* × *trabutii* (82.9 MPa ± 17) had the highest bending strength with respect to the other species. *Melia azedarach* (77.6 MPa ± 19) also displayed relatively high MOR values. *Eucalyptus occidentalis* (64.1 MPa ± 17) and *Eucalyptus bridgesiana* (59.6 MPa ± 11) are at intermediate levels, while *Eucalyptus camaldulensis* (52.7 MPa ± 7) shows generally lower values. The lowest MOR value was found in *Paulownia tomentosa* (31.9 MPa ± 4), characterised by a distribution concentrated on lower values and with relatively reduced variability compared to eucalypts.

Similarly, species significantly affected MOR ($F(5, 114) = 31.54$, $p < 0.001$; $\omega^2 = 0.560$; Table 2). Tukey's HSD test (Table 5) showed the highest MOR for *Eucalyptus* × *trabutii* ("a"), which did not differ significantly from *Melia azedarach* ("ab"). *Eucalyptus occidentalis* ("bc") overlapped with *Melia azedarach* and with the lower group including *Eucalyptus camaldulensis* and *Eucalyptus bridgesiana* (both "c"). Finally, *Paulownia tomentosa* formed a distinct lowest group ("d").

Van Duong and Ridley-Ellis [30] reported a static modulus of elasticity (MOE_s) of 8750 MPa and a modulus of rupture (MOR) of 83.9 MPa for 10-year-old *Melia azedarach plantation* wood in Vietnam. *Melia azedarach* showed a higher MOE (11,583 MPa ± 2273) than the material analysed in the present study, but a slightly lower MOR (77.6 MPa ± 19). This indicates comparable bending strength but greater stiffness in the material analysed here.

Tamantini et al. [32] reported a modulus of rupture (MOR) of 84.4 MPa for *Eucalyptus camaldulensis* obtained from windbreak strips in Tarquinia (central Italy), while, for the same species, Serenini et al. [29] reported a modulus of elasticity (MOE_s) of 10,978 MPa and a modulus of rupture (MOR) of 43.35 MPa in a 5-year-old plantation in Mato Grosso (Brazil). Compared to the previous studies, the present study showed a lower modulus of rupture but higher modulus of elasticity for *Eucalyptus camaldulensis*. Amer et al. [31] reported a modulus of elasticity (MOE_s) of 11,577 MPa and a modulus of rupture (MOR) of 65.81 MPa for the specimens of *Eucalyptus camaldulensis*, and values of 10,275 MPa and 54.41 MPa, respectively, for the MOE_s and MOR of *Eucalyptus grandis*. Ferreira et al. [41] reported a MOE_s of 7396 MPa and a MOR of 71.20 MPa for the conventional plantation of

Eucalyptus urophylla × *Eucalyptus grandis*. In contrast, in the treatment accounting for sun exposure, they obtained 9454 MPa and 78.13 MPa, respectively.

Ivaniuk et al. [40] reported a modulus of elasticity (MOE_s) of 5200 MPa and a modulus of rupture (MOR) of 26 MPa, on specimens of *Paulownia tomentosa*. Barbu et al. [24], by studying a 7-year-old *Paulownia tomentosa* × *elongata* plantation in Serbia and assessing wood properties at different stem heights, reported a MOE_s of 4123 MPa and a MOR of 33.9 MPa at 0–1 m, while at 4.5–6 m they obtained 4941 MPa and 41.8 MPa, respectively. Compared with those results, the present study showed slightly higher stiffness and a MOR within a broadly comparable range, confirming the relatively low but consistent bending performance of *Paulownia tomentosa* wood.

The differences observed in MOE_s and MOR across species can be attributed to variations in wood density and anatomical structure. These factors are known to play a significant role in determining bending stiffness and strength. In this regard, the lower performance recorded for *Paulownia tomentosa* is consistent with its lower wood density.

3.5. Compression Strength

Compression strength parallel to the grain showed clear differences between species (Figure 3). *Eucalyptus* × *trabutii* (46 MPa ± 2) achieved the highest values compared to the other species. *Eucalyptus occidentalis* (41.7 MPa ± 5) achieved slightly lower but still high values. *Melia azedarach* (41.7 MPa ± 3) and *Eucalyptus bridgesiana* (40.2 MPa ± 3) showed intermediate and rather similar levels, while *Eucalyptus camaldulensis* (39.3 MPa ± 3) is inclined to present lower average values. *Paulownia tomentosa* (19.9 MPa ± 3) was clearly distinct from the other species, with the lowest resistances.

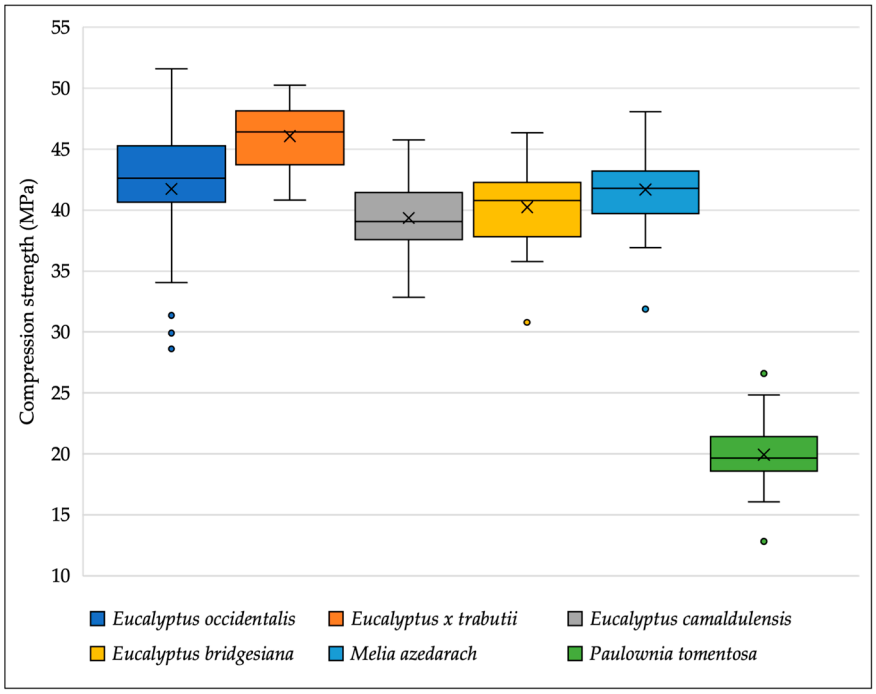

Figure 3. Compression strength of investigated species. Coloured dots represent outliers.

Compression strength parallel to grain differed significantly among species (one-way ANOVA: F (5, 174) = 196.44, $p < 0.001$), with a very large effect size ($\omega^2 = 0.844$; Table 2). Tukey's HSD (Table 6) indicated that *Eucalyptus* × *trabutii* showed the highest compressive strength ("a"), *Paulownia tomentosa* the lowest ("c"), whereas the remaining species (*Eucalyptus occidentalis*, *Eucalyptus camaldulensis*, *Eucalyptus bridgesiana*, and *Melia azedarach*) did not differ significantly from each other and formed an intermediate group ("b").

Table 6. Mean values, standard deviations, and statistical comparison of compression strength.

Tree Species	Compression Strength (MPa) Mean ± SD
Eucalyptus occidentalis	41.73 ± 5.59 b
Eucalyptus × *trabutii*	46.07 ± 2.87 a
Eucalyptus camaldulensis	39.35 ± 3.16 b
Eucalyptus bridgesiana	40.23 ± 3.19 b
Melia azedarach	41.69 ± 3.25 b
Paulownia tomentosa	19.93 ± 2.78 c

Note: Compression strength values sharing the same letter are not significantly different (Tukey's HSD, $\alpha = 0.05$).

Tamantini et al. [32] reported a mean compressive strength of 49.4 MPa parallel to the grain for *Eucalyptus camaldulensis* specimens obtained from windbreak strips in Tarquinia, central Italy. Serenini et al. [29] measured an average compressive strength of 43.35 MPa parallel to the grain for the same species in 5-year-old plantations in Mato Grosso, Brazil, providing a comparable reference value for fast-grown material. In contrast, Amer et al. [31] reported lower values of 30.11 MPa and 26.30 MPa for *E. camaldulensis* and *E. grandis* specimens, respectively, with a moisture content of 12%, highlighting the influence of clone/species and testing conditions on outcomes. Overall, the value obtained in the present study for *Eucalyptus camaldulensis* can therefore be considered intermediate in comparison with previous reports.

Considering *Melia azedarach*, Herawati et al. [43] had determined a compression strength of 28 MPa from plantations in North Sumatra. Comparing with the present study, the value observed here for *Melia azedarach* (41.7 MPa ± 3) is markedly higher, indicating greater resistance under compression parallel to the grain.

Regarding *Paulownia tomentosa*, Ivaniuk et al. [40] reported a compression strength of 22 MPa. Similarly, Barbu et al. [24] in Serbia found compression strengths of 19.41 MPa at 0–1 m and 23.41 MPa at 4.5–6 m, suggesting a modest improvement in compression performance with height along the stem. The value obtained in the present study for *Paulownia tomentosa* (19.9 MPa ± 3) is very close to those reported in the literature, confirming the generally compressive performance, even in a Mediterranean plantation.

As evidenced in the earlier discussion concerning the MOE_s and MOR tests, the ranking in compression strength is largely determined by species-specific variations in wood density and structural organisation. Consequently, the higher compression strength values observed for *Eucalyptus* × *trabutii*, coupled with the intermediate performance of the other *Eucalyptus* species and *Melia azedarach*, likely reflect a denser wood structure. Conversely, the significantly lower values recorded for *Paulownia tomentosa* are consistent with its lower wood density.

3.6. Relationship Between Dynamic and Static Modulus of Elasticity

To evaluate the agreement between non-destructive and destructive estimates of the modulus of elasticity, the relationship between the dynamic modulus (MOE_d, obtained from stress-wave measurements) and the static modulus (MOE_s, obtained from bending tests) was analysed across paired observations (Figure 4). MOE_d was positively associated with MOE_s ($MOE_s = 1.0106 \cdot MOE_d + 757.04$; $R^2 = 0.41$; $r \approx 0.65$; $p < 0.001$), indicating that higher dynamic values generally corresponded to higher static modulus of elasticity. However, the coefficient of determination indicates only moderate predictive ability, meaning that MOE_d explained less than half of the variation in MOE_s. Part of the observed dispersion may be related to the different moisture conditions under which the two properties were determined since MOE_d was estimated on standing trees in green condition, whereas MOE_s was measured on laboratory specimens conditioned to approximately 12% moisture content.

Although its predictive accuracy for estimating MOE_d remains moderate, particularly in the intermediate performance range, the use of stress-wave tools can still be considered a practical non-destructive tool for preliminary screening and ranking of fast-growing species under the studied plantation conditions.

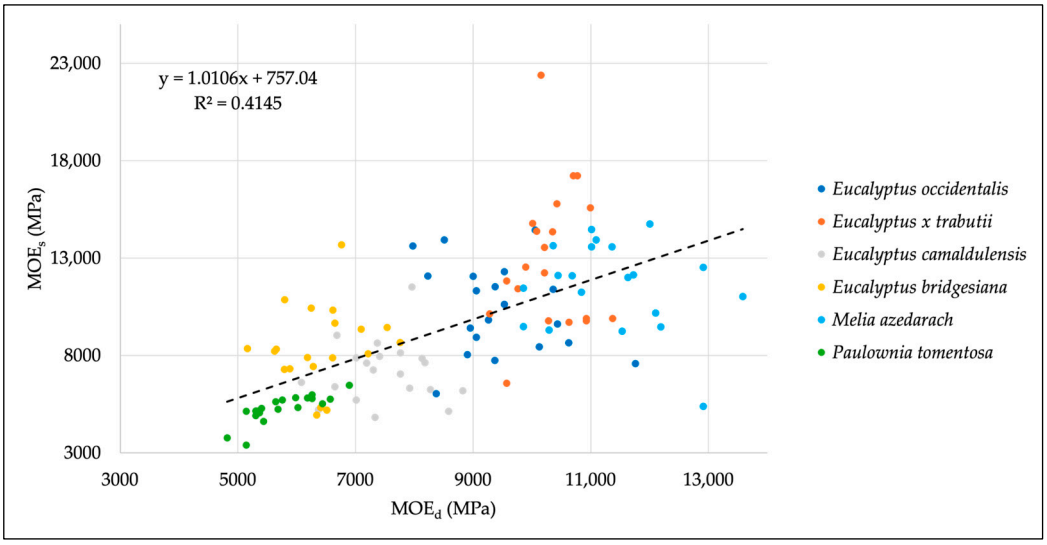

Figure 4. Relationship between dynamic modulus of elasticity (MOE_d) and static modulus of elasticity (MOE_s) across paired observations. The dashed line represents the overall linear regression (equation and R^2 shown in the plot); points are colour-coded by species.

Consistently, stress-wave measurements distinguished species with higher MOE_d (e.g., *Melia azedarach* and *Eucalyptus* × *trabutii*) from lower-MOE_d material (e.g., *Paulownia tomentosa*), in agreement with the ranking obtained from static bending properties. This suggests that, in Mediterranean fast-growing plantations, MOE_d can support early selection decisions and contribute to defining species- or clone-oriented management strategies and end-use pathways in short-rotation forestry and agroforestry systems.

Fast-growing species are often perceived as having inferior mechanical performance compared with slower-growing hardwoods; however, our results highlight substantial variability within this group. Some species combine rapid growth with comparatively high modulus of elasticity and bending strength, whereas others provide lighter wood more suitable for non-structural applications. Under these conditions, MOE_d measurements represent a valuable tool to capture this variability and to better match species and clones to appropriate end-uses.

4. Conclusions

Based on the results obtained, clear interspecific differences emerged in the mechanical performances of the investigated fast-growing, non-native hardwoods cultivated under Mediterranean conditions. Both standing-tree stress-wave measurements (MOE_d) and laboratory tests (MOE_s, MOR, and compression strength) revealed marked variability in stiffness and resistance among species, highlighting the need for species-specific grading and end-use allocation. The positive relationship observed between MOE_d and MOE_s indicates that, although its predictive accuracy remains debatable, stress-wave testing can serve as a practical, rapid tool for screening and ranking plantation material before processing, supporting early decision-making in SRF and agroforestry systems. Overall, the results demonstrate that "fast-growing species" does not imply uniformly low wood quality: within the studied plantations, certain species/clones combine rapid growth with comparatively high stiffness and strength, while others offer lower-density wood better

suited for alternative end-uses. These results provide comparative evidence to guide species/clonal selection and to better match plantation resources to targeted value chains in Mediterranean environments. Future work should expand sampling across sites and ages and include additional wood quality indicators (e.g., defects, knot influence, and durability traits) to refine end-use allocation.

Author Contributions: Conceptualisation, A.R.P., A.Z. and S.F.P.; methodology, A.R.P., A.Z. and S.F.P.; validation, A.R.P., A.L.M. and R.P.; formal analysis, A.R.P., A.Z. and S.F.P.; investigation, A.Z. and S.F.P.; resources, A.R.P.; data curation, A.Z.; writing—original draft preparation, A.R.P. and A.Z.; writing—review and editing, A.R.P., A.L.M. and R.P.; visualisation, A.L.M., A.R.P. and A.Z.; supervision, A.R.P. project administration, A.R.P. and A.Z.; funding acquisition, A.R.P. All authors have read and agreed to the published version of the manuscript.

Funding: This work was supported by the course "Agricultural, Food and Forestry Science" of the Mediterranean University of Reggio Calabria (Italy)—XXXIX cycle and by the inter-institutional agreement between the Mediterranean University of Reggio Calabria (Italy) and ARSAC (Regional Company for the Development of Calabrian Agriculture). The research was carried out within framework of the Ministry of University and Research (MUR) initiative "Departments of Excellence" (Law 232/2016) DAFNE Project 2023-27 "Digital, Intelligent, Green and Sustainable (acronym: D.I.Ver.So)".

Data Availability Statement: The data supporting the conclusions of this article will be made available by the authors on request.

Acknowledgments: Authors would like to thank Roberto Bonofiglio for supporting logistically this study.

Conflicts of Interest: The authors declare no conflicts of interest.

References

1. Akpan, E.I.; Wetzel, B.; Friedrich, K. Eco-friendly and sustainable processing of wood-based materials. *Green Chem.* **2021**, *23*, 2198–2232. [CrossRef]
2. Genco, G.; Pelosi, C.; Santamaria, U.; Lo Monaco, A.; Picchio, R. Study of colour change due to accelerated sunlight exposure in consolidated wood samples. *Wood Res.* **2011**, *56*, 511–524.
3. FAO. FAOSTAT Forestry Production and Trade Domain. 2021. Available online: http://www.fao.org/faostat/en/#data/FO (accessed on 26 January 2026).
4. Peng, L.; Searchinger, T.D.; Zionts, J.; Waite, R. The carbon costs of global wood harvests. *Nature* **2023**, *620*, 110–115. [CrossRef]
5. Forster, E.J.; Styles, D.; Healey, J.R. Temperate forests can deliver future wood demand and climate-change mitigation dependent on afforestation and circularity. *Nat. Commun.* **2025**, *16*, 3872. [CrossRef]
6. FAO. *Global Forest Sector Outlook 2050: Assessing Future Demand and Sources of Timber for a Sustainable Economy—Background Paper for the State of the World's Forests 2022*; FAO Forestry Working Paper, No. 31; FAO: Rome, Italy, 2022; pp. 1–115. [CrossRef]
7. Verkerk, P.J.; Hassegawa, M.; Van Brusselen, J.; Cramm, M.; Chen, X.; Maximo, Y.I.; Koç, M.; Lovrić, M.; Tegegne, Y.T. *Forest Products in the Global Bioeconomy: Enabling Substitution by Wood-Based Products and Contributing to the Sustainable Development Goals*; FAO: Rome, Italy, 2022; pp. 1–148. [CrossRef]
8. FAO. *The State of the World's Forests 2024—Forest-Sector Innovations Towards a More Sustainable Future*; FAO: Rome, Italy, 2024; pp. 1–104. [CrossRef]
9. Di Matteo, G.; Sperandio, G.; Verani, S. Field performance of poplar for bioenergy in southern Europe after two coppicing rotations: Effects of clone and planting density. *Iforest-Biogeosci. For.* **2012**, *5*, 224. [CrossRef]
10. Picchio, R.; Tavankar, F.; Rafie, H.; Kivi, A.R.; Jourgholami, M.; Lo Monaco, A. Carbon storage in biomass and soil after mountain landscape restoration: *Pinus nigra* and *Picea abies* plantations in the Hyrcanian Region. *Land* **2022**, *11*, 422. [CrossRef]
11. Rockwood, D.L.; Naidu, C.V.; Carter, D.R.; Rahmani, M.; Spriggs, T.A.; Lin, C.; Alker, G.R.; Isebrands, J.G.; Segrest, S.A. Short-rotation woody crops and phytoremediation: Opportunities for agroforestry? *Agrofor. Syst.* **2004**, *61*, 51–63. [CrossRef]
12. Vanbeveren, S.P.; Ceulemans, R. Biodiversity in short-rotation coppice. *Renew. Sustain. Energy Rev.* **2019**, *111*, 34–43. [CrossRef]
13. Lindegaard, K.N.; Adams, P.W.; Holley, M.; Lamley, A.; Henriksson, A.; Larsson, S.; von Engelbrechten, H.G.; Esteban Lopez, G.; Pisarek, M. Short rotation plantations policy history in Europe: Lessons from the past and recommendations for the future. *Food Energy Secur.* **2016**, *5*, 125–152. [CrossRef] [PubMed]

14. Cerasoli, S.; Caldeira, M.C.; Pereira, J.S.; Caudullo, G.; de Rigo, D. Eucalyptus globulus and other eucalypts in Europe: Distribution, habitat, usage and threats. In *European Atlas of Forest Tree Species*; San-Miguel-Ayanz, J., de Rigo, D., Caudullo, G., Houston Durrant, T., Mauri, A., Eds.; Publications Office of the EU: Luxembourg, 2016; p. e01b5bb+.
15. Scarascia-Mugnozza, G.; Sabatti, M.; Paris, P. La produzione di biomassa da colture arboree: Realtà italiana e prospettive. In *Nuove Frontiere Dell'arboricoltura Italiana*; Silverio, S., Ed.; Gruppo Perdisa: Bologna, Italy, 2007; pp. 517–533. (In Italian)
16. Minini, D.; Amaral Reis, C.; de Moura Borges, M.D.; Pontes Teixeira das Chagas, K.; da Silva Lins, T.R.; Gonzalez de Cademartori, P.H.; Vidaurre, G.B.; Nisgoski, S. A review on the quality of wood from agroforestry systems. *Agrofor. Syst.* **2024**, *98*, 715–737. [CrossRef]
17. Zalesny, R.S., Jr.; Barzagli, A.; Caldwell, B.; Minotta, G.; Nervo, G.; Paris, P.; Rogers, E.R.; Salbitano, F. (Eds.) *Innovative Practices in the Sustainable Management of Fast-Growing Trees—Lessons Learned from Poplars and Willows and Other Experiences with Fast-Growing Trees Around the World*; FAO: Rome, Italy, 2025; 192p. [CrossRef]
18. Wilson, M.H.; Lovell, S.T. Agroforestry—The next step in sustainable and resilient agriculture. *Sustainability* **2016**, *8*, 574. [CrossRef]
19. Ramachandran Nair, P.K.; Kumar, B.M.; Nair, V.D. *An Introduction to Agroforestry: Four Decades of Scientific Developments*, 2nd ed.; Springer Nature: Cham, Switzerland, 2021; pp. 1–649. [CrossRef]
20. Waheed, M.; Arshad, F.; Fatima, K.; Jabeen, A.; Al-Andal, A.; Ugli, A.A.F.; Nurullayeva, B.; Khujaniyozova, O. Optimizing agroforestry systems through traditional ecological knowledge: A sustainable model for tree species selection in semi-arid lowland region. *Agrofor. Syst.* **2025**, *99*, 176. [CrossRef]
21. Nicolescu, V.N.; Rédei, K.; Vor, T.; Bastien, J.C.; Brus, R.; Benčať, T.; Štefančik, I. A review of black walnut (*Juglans nigra* L.) ecology and management in Europe. *Trees* **2020**, *34*, 1087–1112. [CrossRef]
22. Roberti, G.; Herzog, F.; Jäger, M.; Kay, S. Temperate agroforestry for tree carbon storage in Switzerland: 10 years of biophysical and social monitoring. *Clim. Smart Agric.* **2025**, *2*, 100055. [CrossRef]
23. Sutapa, J.P.G. Properties and utilization possibilities of Mindi *(Melia azedarach* L.) wood from agroforestry plantation. In *Proceedings of the 3rd International Conference in Agroforestry (ICAF) "Adopting Modern Agroforestry Toward Smart Social Forestry Program", Yogyakarta, Indonesia, 16–17 October 2019*; IOP Publishing Purpose-led Publishing: Philadelphia, PA, USA, 2020; Volume 449, p. 012026. [CrossRef]
24. Barbu, M.C.; Tudor, E.M.; Buresova, K.; Petutschnigg, A. Assessment of Physical and Mechanical Properties Considering the Stem Height and Cross-Section of *Paulownia tomentosa* (Thunb.) Steud. *x elongata* (S.Y.Hu) Wood. *Forests* **2023**, *14*, 589. [CrossRef]
25. Lima, M.D.R.; Moraes, L.G.; Silva, R.d.C.C.; Barros Junior, U.d.O.; Bufalino, L.; Soares, A.A.V.; Assis-Pereira, G.; Gonçalves, D.d.A.; Tomazello-Filho, M.; Protásio, T.d.P. Tachigali vulgaris energy forests: Understanding spacing, age, and stem type effects on tree growth patterns and wood density. *New For.* **2023**, *54*, 491–513. [CrossRef]
26. Liu, C.L.C.; Kuchma, O.; Krutovsky, K.V. Mixed-species versus monocultures in plantation forestry: Development, benefits, ecosystem services and perspectives for the future. *Glob. Ecol. Conserv.* **2018**, *15*, e00419. [CrossRef]
27. Zhai, B.; Sun, M.; Shen, X.; Zhu, Y.; Li, G.; Du, S. Effects of Stand Density on Growth, Soil Water Content and Nutrients in Black Locust Plantations in the Semiarid Loess Hilly Region. *Sustainability* **2024**, *16*, 376. [CrossRef]
28. Papandrea, S.F.; Proto, A.R.; Cataldo, M.F.; Zimbalatti, G. Comparative Evaluation of Inspection Techniques for Decay Detection in Urban Trees. *Environ. Sci. Proc.* **2021**, *3*, 14. [CrossRef]
29. Serenini, L., Jr.; De Melo, R.R.; Stangerlin, D.M.; Pimenta, A.S. Wood quality of six Eucalyptus clones planted in northern Mato Grosso State, Brazil. *Wood Res.* **2020**, *65*, 543–554. [CrossRef]
30. Van Duong, D.; Ridley-Ellis, D. Estimating mechanical properties of clear wood from ten-year-old *Melia azedarach* trees using the stress wave method. *Eur. J. Wood Prod.* **2021**, *79*, 941–949. [CrossRef]
31. Amer, M.; Kabouchi, B.; Rahouti, M.; Famiri, A.; Fidah, A.; El Alami, S. Mechanical properties of clonal eucalyptus wood. *Int. J. Thermophys.* **2021**, *42*, 20. [CrossRef]
32. Tamantini, S.; Peruzzo, A.; Bergamasco, S.; Scarnati, L.; Romagnoli, M. Physical and morphological characterization of eucalyptus wood (*Eucalyptus camaldulensis* Dehnh.) from seaside windbreaks belts in Central Italy. *Eur. J. Wood Prod.* **2025**, *83*, 149. [CrossRef]
33. Nocetti, M.; Brunetti, M.; Criscuoli, I.; Mazzanti, P.; Murrone, P.; Stefanini, F.M.; Goli, G. Technological properties of Paulownia and mixed poplar-Paulownia plywood. *Eur. J. Wood Wood Prod.* **2025**, *83*, 142. [CrossRef]
34. *ISO 13061-2:2014*; Physical and Mechanical Properties of Wood—Test Methods for Small Clear Wood Specimens—Part 2: Determination of Density for Physical and Mechanical Tests. International Organization of Standardization (ISO): Geneva, Switzerland, 2014.
35. *ISO 13061-1:2014*; Physical and Mechanical Properties of Wood—Test Methods for Small Clear Wood Specimens—Part 1: Determination of Moisture Content for Physical and Mechanical Tests. International Organization of Standardization (ISO): Geneva, Switzerland, 2014.
36. *ISO 13061-16:2025*; Physical and Mechanical Properties of Wood—Test Methods for Small Clear Wood Specimens—Part 16: Determination of Volumetric Swelling. International Organization of Standardization (ISO): Geneve, Switzerland, 2025.

37. *ISO 13061-14:2024*; Physical and Mechanical Properties of Wood—Test Methods for Small Clear Wood Specimens—Part 14: Determination of Volumetric Shrinkage. International Organization of Standardization (ISO): Geneve, Switzerland, 2024.
38. *EN 408:2010+A1*; Timber Structures—Structural Timber and Glued Laminated Timber—Determination of Some Physical and Mechanical Properties. European Committee for Standardization: Brussels, Belgium, 2012.
39. *ISO 13061-17:2022*; Physical and Mechanical Properties of Wood—Test Methods for Small Clear Wood Specimens—Part 17: Determination of Ultimate Stress in Compression Parallel to Grain. International Organization of Standardization (ISO): Geneva, Switzerland, 2022.
40. Ivaniuk, A.; Zayachuk, V.; Lysiuk, R.; Kharachko, T.; Lisoviy, M. Physical and mechanical properties of *Paulownia tomentosa* (Thunb.) Steud. wood under the conditions of the Western Forest-Steppe of Ukraine. *For. Ideas* **2023**, *1*, 168–190.
41. Ferreira, M.D.; Rodolfo de Melo, R.; Tonini, H.; Pimenta, A.S.; Gatto, D.A.; Beltrame, R.; Stangerlin, D.M. Physical–mechanical properties of wood from a eucalyptus clone planted in an integrated crop-livestock-forest system. *Int. Wood Prod. J.* **2020**, *11*, 12–19. [CrossRef]
42. McComb, J.A.; Meddings, R.A.; Siemon, G.; Davis, S. Wood density and shrinkage of five-year-old *Eucalyptus camaldulensis* × *E. globulus hybrids*: Preliminary assessment. *Aust. For.* **2004**, *67*, 236–239. [CrossRef]
43. Herawati, E.; Hartono, R.; Sinaga, H.M.M. Physical and mechanical properties of four wood species from community forests in Binjai Regency, North Sumatra. In *Proceedings of the 3rd International Conference on Natural Resources and Technology 24–25 August 2021, Medan, Indonesia*; IOP Publishing Purpose-led Publishing: Philadelphia, PA, USA, 2021; Volume 912, p. 012024. [CrossRef]